

Clinical Application of Readout-Segmented (RS)-EPI for Diffusion-Weighted Imaging in Pediatric Brain

S. J. Holdsworth¹, K. Yeom¹, S. Skare¹, P. D. Barnes¹, and R. Bammer¹

¹Radiology, Stanford University, Palo Alto, CA, United States

Introduction: Readout-segmented (RS)-EPI [1] has been suggested as an alternative approach to EPI for high resolution diffusion-weighted imaging (DWI) with reduced distortions. Here we implemented GRAPPA-accelerated RS-EPI DWI on 35 pediatric patients at 3T. We compared these images with standard accelerated (ASSET) EPI DWI used routinely for clinical studies at our pediatric hospital.

Methods: RS-EPI and EPI images were acquired on 35 pediatric patients using a 3T whole-body system (GE DVMR750) and an 8-channel head coil. The following parameters were used: FOV=20cm, slthck=4mm, TR=3s, one $b=0$ and three diffusion directions with $b=1000 \text{ s/mm}^2$ (xyz encoding). RS-EPI used a twice-refocused diffusion preparation with a matrix size = 192^2 , 7 segments (width=64, overlap factor=57%), acceleration factor $R=3$, NEX=3, and a scan time of 4:12min. GRAPPA and ghost calibration were performed on the multi-shot data, thus no separate calibration scan was acquired. Data were reconstructed as described elsewhere [2]. The routine ASSET-accelerated EPI sequence used for comparison: matrix size= 128^2 , $R=2$, one $b=0$ and three diffusion directions with $b=1000 \text{ s/mm}^2$ (xyz encoding), and a scan time of 50s. A pediatric neuroradiologist evaluated the DW images, scoring them in terms of resolution, distortion level, SNR, lesion conspicuity, and diagnostic confidence as follows: 1 – non-diagnostic, 2 – poor, 3 – acceptable, 4 – standard, 5 – above average, 6 – good, 7 – outstanding. First the images were scored independently, followed by a reevaluation of the RS-EPI images with the datasets viewed together. Finally, an overall preference was selected.

Results: Fig. 1 shows the average scores calculated across 35 patients for EPI, RS-EPI, and EPI vs RS-EPI. The RS-EPI dataset was preferred overall in all except for two patients due to the presence of phase artifacts on RS-EPI arising from pulsatile brain motion. In 12 patients, the EPI scans suffered from mild-to-severe ‘worm-like’ artifacts also arising from brain motion (though not accounted for when considering the final preference). RS-EPI identified a lesion not identified by EPI in one patient (small subdural empyema, Fig. 2); more accurately defined the extent and structure of lesions, such as a cystic encephalomalacia (Fig. 3a) and a clival chordoma (Fig. 3b); had improved additional lesion localization in one patient (Leigh's disease, Fig. 4); and correctly identified a false positive lesion seen on EPI on another patient (Moya Moya disease, Fig. 5). RS-EPI also demonstrated exquisite anatomic detail at the cortical-subcortical levels, brainstem, temporal and inferior frontal lobes, skull base, orbits, naso-ethmoid, and the cranial nerves – all of which were more difficult to assess on EPI. Overall, the RS-EPI had significantly improved diagnostic confidence.

Discussion & Conclusion: Averaged over 34 patients, RS-EPI out-performed the product ASSET EPI sequence (Fig. 1). RS-EPI was chosen as the overall preference for all but two patients due to the presence of phase artifacts on DWI. Note that these artifacts were later removed by increasing the triangular window used for phase correction to the full k -space radius (data not shown). In conclusion, RS-EPI may be a useful alternative to EPI for DWI for evaluating lesions such as hypoxic-ischemic brain injury, diffuse axonal injury, tumors, dermoid/epidermoid, and skull base/orbital pathology. While some of the imaging parameters of the two sequences were not identical, this study shows the importance of both resolution and decreased distortions in the clinics, which can be accomplished by a combination of parallel imaging and alternative k -space trajectories such as RS-EPI. Aside from SNR, increasing the number of averages for EPI (to match the scan time of the RS-EPI) is not expected to change the outcome of this study as it is primarily the resolution and distortion improvements that led to increased lesion conspicuity and diagnostic confidence.

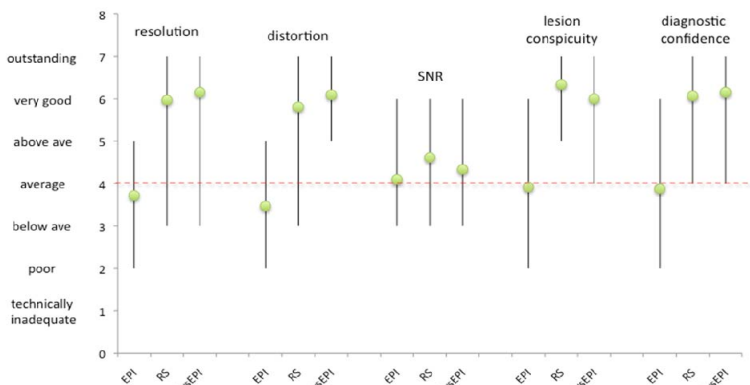


Fig 1. Comparison between the routine ASSET-accelerated EPI sequence and our implementation of RS-EPI in terms of 5 categories averaged over 35 patients.

References: [1] Porter D. ISMRM 2008;3262. [2] Holdsworth S. MRM 2009;62 (early view).

Acknowledgements: This work was supported in part by the NIH (1R01 EB008706, 1R01 EB008706S1, 5R01 EB002711, 1R01 EB006526, 1R21 EB006860), the Center of Advanced MR Technology at Stanford (P41RR09784), Lucas Foundation, Oak Foundation, and the Swedish Research Council (K2007-53P-20322-01-4). Special thanks to Serman Lim, Alfred Barikdar, Allan White, Young Chang, Harold Estrada, Liz Ellison, and Abbie Bird and for their assistance with the patient studies.

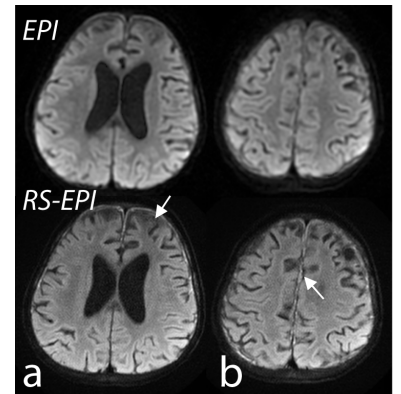


Fig 2. Patient presenting with subdural empyema. (a) Abscess depicted with greater diagnostic confidence on RS-EPI. (b) Pus present along falx on RS-EPI not well seen on EPI.

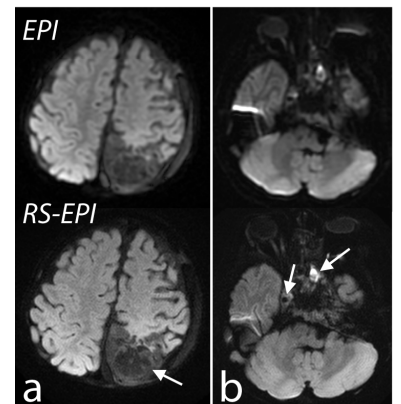


Fig 3. Patient presenting with (a) cystic encephalomalacia and (b) cellular tumor (anaplastic chordoma). RS-EPI demonstrates ‘cystic’ encephalomalacic changes with higher resolution. RS-EPI also results in improved detail at the skull base (cavernous sinus, Meckel's cave, clivus, petrous apices).

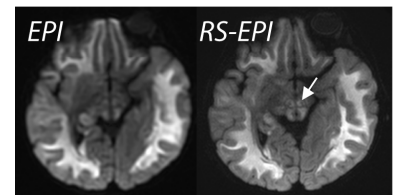


Fig 4. Patient with Leigh's disease. RS-EPI shows exquisite resolution at the level of the brain stem, specifically in the dorsal midbrain. The red nucleus is also better defined on RS-EPI (white arrow).

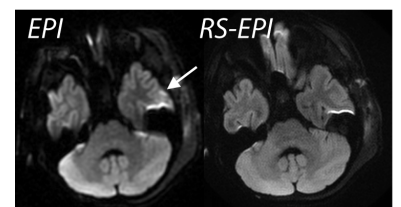


Fig 5. Patient with Moya-Moya disease presents with possible infarct or blood product at the surgical site on EPI (white arrow). The absence of this distortion artifact on RS-EPI makes this confidently negative.